

Electron capture and emission properties of interface states in thermally oxidized and NO-annealed SiO₂/4H-SiC

X. D. Chen,^{1,a)} S. Dhar,² T. Isaacs-Smith,³ J. R. Williams,³ L. C. Feldman,^{2,b)} and P. M. Mooney¹

¹*Department of Physics, Simon Fraser University, Burnaby, B.C. V5A 1S6, Canada*

²*Department of Physics and Astronomy, Vanderbilt University, Nashville, Tennessee 37235, USA*

³*Physics Department, Auburn University, Auburn, Alabama 36849, USA*

(Received 6 September 2007; accepted 24 November 2007; published online 5 February 2008)

Postoxidation annealing in nitric oxide (NO) results in a significant reduction of electronic states at SiO₂/4H-SiC interfaces. Measurements of electron trapping dynamics at interface states in both thermally oxidized and NO annealed SiO₂/4H-SiC interfaces were performed using constant-capacitance deep level transient spectroscopy (CCDLTS) and double-CCDLTS. We show that the interface state density in as-oxidized samples consists of overlapping distributions of electron traps that have distinctly different capture cross sections. The dominant trap distributions, centered at $E_c - 0.24$ eV with $\sigma \sim 7 \times 10^{-19}$ cm², and at $E_c - 0.46$ eV with $\sigma \sim 4 \times 10^{-17}$ cm² are passivated by NO annealing. The remaining interface states all have capture cross sections in the range $10^{-19} - 10^{-21}$ cm². © 2008 American Institute of Physics. [DOI: 10.1063/1.2837028]

I. INTRODUCTION

The electrical and physical properties of silicon carbide (SiC) and its ability to form insulating SiO₂ layers by thermal oxidation make it a promising material for high power, high-temperature, and high-frequency metal-oxide-semiconductor field effect transistors (MOSFETs).¹⁻³ The most favorable SiC polytype for such devices is 4H-SiC because of its large band gap energy, 3.26 eV, and bulk electron mobility of ~ 800 cm²/V s. Historically, however, the development of 4H-SiC MOSFETs has been hindered by the high density of interface states (D_{it}) at the SiO₂/4H-SiC interface, which results in a reduced electron mobility of < 10 cm²/V s in n -channel inversion layers.^{1,3-5} Interfacial nitridation via postoxidation annealing in nitric oxide (NO) results in the incorporation of about a monolayer of N ($\sim 10^{15}$ cm⁻²) at or near the interface and reduces D_{it} near the conduction band edge of 4H-SiC by almost an order of magnitude. This in turn leads to a significantly improved effective channel mobility in n -channel 4H-SiC MOSFETs.^{2,3,6} While nitridation has been established as the most efficient oxide processing scheme for SiC devices, the N related trap passivation mechanism and the electronic nature of residual traps at nitrided SiO₂/4H-SiC interfaces remain unclear.

In this article, we present new insights on the capture and emission properties of electronic states at as-oxidized and nitrided interfaces using constant-capacitance deep level transient spectroscopy (CCDLTS) and double-CCDLTS measurements, methods that have been used effectively to study interface states in SiO₂/Si MOS structures.^{7,8} We show that the D_{it} detected by CCDLTS in as-oxidized samples consists

primarily of three overlapping distributions of interface states, distinguished by their different capture cross sections, that are passivated by NO annealing. The capture cross sections of the remaining interface states in nitrided samples are in the range $10^{-21} - 10^{-19}$ cm², much smaller than values reported for SiO₂/Si interfaces.⁹

II. EXPERIMENT

Samples used for this work are 5 mm \times 5 mm pieces diced from an 8° off-axis (0001) Si face n -type 4H-SiC wafer with 10 μ m epilayer doped with nitrogen at 5.5×10^{15} cm⁻³. Dry oxidation was performed at 1150 °C for 8 h followed by annealing at 1150 °C for 30 min in Ar to grow SiO₂ layers with thickness of ~ 60 nm. Some samples were subsequently annealed in NO for 2 h at 1175 °C. The NO annealing resulted in an additional ~ 2 nm oxide thickness. MOS capacitors were fabricated on both sets of samples. Large area ohmic contacts were made to the backside of the n^+ 4H-SiC substrate, which is N doped at $\sim 10^{19}$ cm⁻³, by evaporating ~ 100 nm of Au. Contacts to the SiO₂ layer were made by evaporating 200 nm-thick Al circular dots having a diameter of 0.5 mm.

Simultaneous high-low frequency capacitance-voltage ($C-V$) measurements at room temperature were performed to verify the reduction in interface state density, D_{it} , near the conduction-band edge associated with NO annealing.²⁻⁴ In addition, the MOS capacitors were characterized using $C-V$ measurements at 1 MHz in the temperature range 300–80 K. CCDLTS and double-CCDLTS measurements,^{7,8} were performed in the same temperature range using a SULA Technologies instrument. For CCDLTS measurements the voltage transient needed to maintain the constant value of the sample capacitance and thus a constant depletion width in the semiconductor is sampled at times t_1 and t_2 after the trap filling pulse. The voltage difference, the CCDLTS signal, is plotted as a function of temperature. For double-

^{a)}Author to whom correspondence should be addressed. Electronic mail: xdchen@sfu.ca.

^{b)}Present address: Inst. Adv. Mat. Dev. and Nanotech., Rutgers University, New Brunswick, NJ 08901, USA.

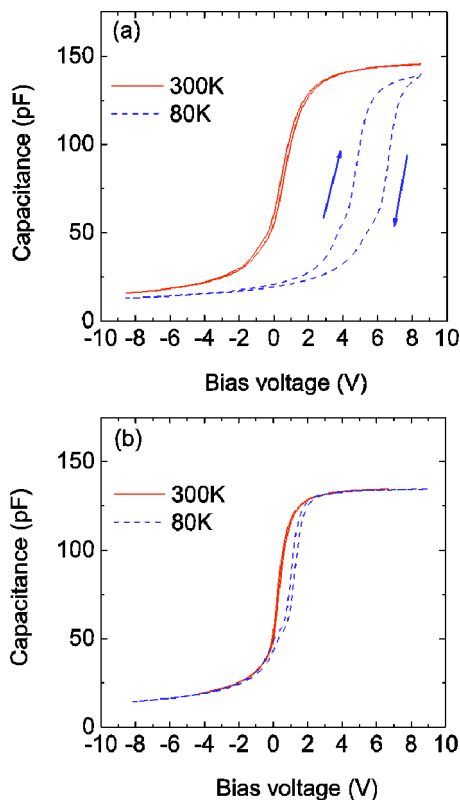


FIG. 1. (Color online) C - V data at 1 MHz for (a) AO and (b) NO $\text{SiO}_2/4\text{H-SiC}$ MOS capacitors.

CCDLTS measurements of interface states a pair of filling pulses having the same duration but slightly different voltages define a narrow energy interval.⁸ The CCDLTS signal is recorded for one of the filling pulses and a differential amplifier provides the difference of the CCDLTS signals for the two filling pulses, the double-CCDLTS signal. The temperature of the double-CCDLTS peak from interface states is expected to shift as the energy window, and therefore the energy position of the sampled traps, changes.⁸ In contrast, single CCDLTS scans do not provide information on the spatial location of the traps.

To evaluate the effect of carrier freeze-out on interface charging during CCDLTS measurements at temperatures below 100 K, the SiO_2 layer was removed from an as-oxidized (AO) sample by HF etching and Schottky contacts were fabricated directly on the 4H-SiC substrate by depositing 600 and 300 μm diameter Ni/Ti/Au dots. The donor concentration from C - V measurements at 300K and 80K shows only a small decrease, from 5.6×10^{15} to 4.1×10^{15} cm^{-3} . Furthermore, no CCDLTS signal was observed for the Schottky diodes demonstrating that the CCDLTS signal for the MOS structures originates entirely from the interface states, not from states in the SiC.

III. RESULTS

A. C - V measurements

Typical C - V curves for AO and NO-annealed (NO) samples measured at 300 and 80 K are shown in Fig. 1. The C - V curves of the AO samples shift toward higher gate voltages with decreasing temperature, indicating that a sig-

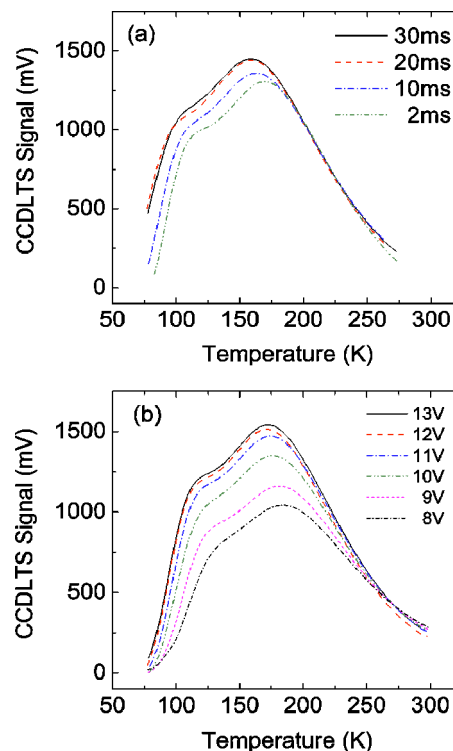


FIG. 2. (Color online) CCDLTS spectra for the AO sample measured with (a) varying filling pulse duration at filling pulse voltage 13 V and (b) varying filling pulse voltage at 20 ms duration. The rate window is 8.6 ms and the constant capacitance is 42 pF.

nificantly higher number of electrons are trapped at $\text{SiO}_2/4\text{H-SiC}$ interface states under low temperature flatband conditions. The shift in the C - V curves for the NO samples in the same temperature range is ~ 10 times smaller than that of the AO sample. Additionally, the hysteresis in the low temperature C - V for opposite voltage sweep directions is significantly smaller for the NO samples than that for the AO samples. These data further demonstrate the significant reduction in carrier trapping at interface states after NO annealing.

B. CCDLTS

Figure 2 shows CCDLTS data for the AO sample. A series of CCDLTS spectra measured with filling pulses of different duration is shown in Fig. 2(a). With increasing filling pulse duration, the CCDLTS spectra become broader in the temperature range 80–100 K and saturate for pulse duration of 20 ms. This indicates that longer pulses are required to fill the shallower interface states. This suggests that the capture cross section of the deeper states observed at higher temperatures is much larger than that of the shallower interface states observed at lower temperatures. The shape of the CCDLTS spectrum suggests the presence of overlapping distributions of at least two types of interface traps, consistent with previous reports on as-oxidized interfaces.^{10–12} Figure 2(b) shows CCDLTS spectra taken with various filling pulse voltages. The CCDLTS signal continues to increase up to a filling pulse of 12 V, consistent with the strong shift of the C - V curve toward positive voltage at low temperature. Thus, to completely fill the interface states, both a filling voltage of 20 ms and at least 12 V is required.

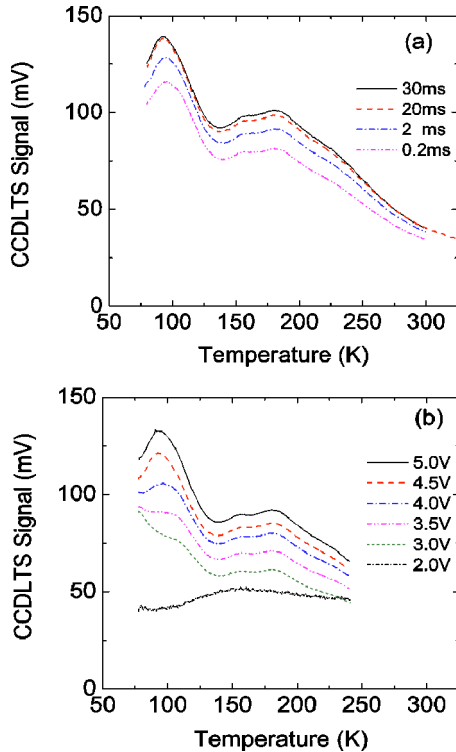


FIG. 3. (Color online) CCDLTS spectra for the NO sample measured with (a) varying filling pulse duration at filling pulse voltage 5 V and (b) with varying filling pulse voltage at 20 ms duration. The rate window is 8.6 ms and the constant capacitance is 18 pF.

Figure 3 shows CCDLTS spectra for the NO sample. We see in Fig. 3(a) that the CCDLTS signal increases over the entire temperature range with increasing filling pulse duration, again saturating at 20 ms. This indicates that, unlike the AO sample, all of the interface states in the NO sample have a similar capture cross section. Figure 3(b) shows that the CCDLTS spectra taken at various filling pulse voltages. The spectrum at 6 V (not shown) overlays that taken at 5 V, showing that the CCDLTS signal saturates at 5 V. Note that the dominant CCDLTS peak at about 100 K increases and shifts to a lower temperature for filling pulses >3 V, suggesting that more than one type of interface trap may be present.

Figure 4 compares the saturated CCDLTS signal intensity for both the AO and NO samples measured with an identical rate window. The CCDLTS intensity of the NO sample is smaller than that of the AO sample by a factor of ~ 10 , again demonstrating the large reduction of the D_{it} in the upper half of the band gap with NO annealing. The dominant interface states for the AO sample appear in the temperature range 100–250 K. For the NO sample, the dominant interface states are found at lower temperature, in the range 80–120 K. In this case also, the presence of peaks in the spectra (indicated by arrows) suggests overlapping distributions of interface states. Note the decrease in the CCDLTS signal at the low end of the temperature range for both samples.

C. Double-CCDLTS

Double-CCDLTS measurements were performed to further investigate the emission and capture kinetics of the in-

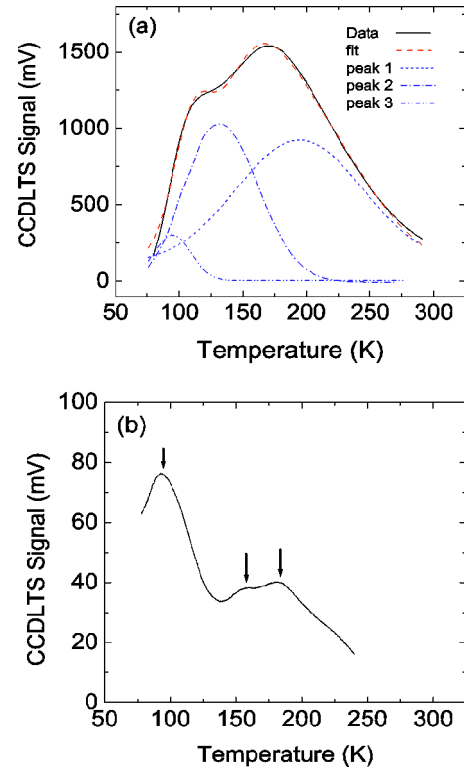


FIG. 4. (Color online) CCDLTS spectra measured for (a) AO and (b) NO $\text{SiO}_2/4\text{H-SiC}$. The filling pulse duration is 20 ms to achieve saturation of the signal and the rate window is 8.6 ms. The constant capacitance is 42 pF and the filling pulse voltage is 13 V for the AO and 18 pF and 5 V for the NO sample.

terface states. Figure 5(a) shows a series of double-CCDLTS scans for the AO sample labeled with the filling pulse voltages used. These scans are grouped according to their characteristics: (1) broad peaks which shift to lower temperature with decreasing filling voltage (4.0–8.0 V); (2) narrower peaks, which also shift to lower temperature and whose amplitude increases and then decreases with decreasing filling voltage (8.0–11.5 V); and (3) peaks at <100 K whose temperature position is fixed and whose intensity decreases with increasing filling voltage (11.5–13 V). The peak shift with increasing filling voltage is expected for interface states.^{7,8} Thus, the fixed peak temperature of the group 3 states is anomalous and suggests that this trap species may not be located precisely at the $\text{SiO}_2/4\text{H-SiC}$ interface. These results indicate that three distinct distributions of interface traps are present in the AO samples. For the NO sample [Fig. 5(b)], we see two groups of peaks: one showing the same anomalous behavior as the group 3 peak in the AO sample, with the peak position independent of the filling voltage (4–5 V), and a second where the peak shifts to lower temperature with decreasing filling voltage (2–4 V). This indicates that at least two types of interface states are present at the $\text{SiO}_2/4\text{H-SiC-SiC}$ interface after nitridation.

D. Activation energy and capture cross section

To measure the emission activation energy and capture cross section of these states, double-CCDLTS scans were taken at various rate windows on both AO and NO samples

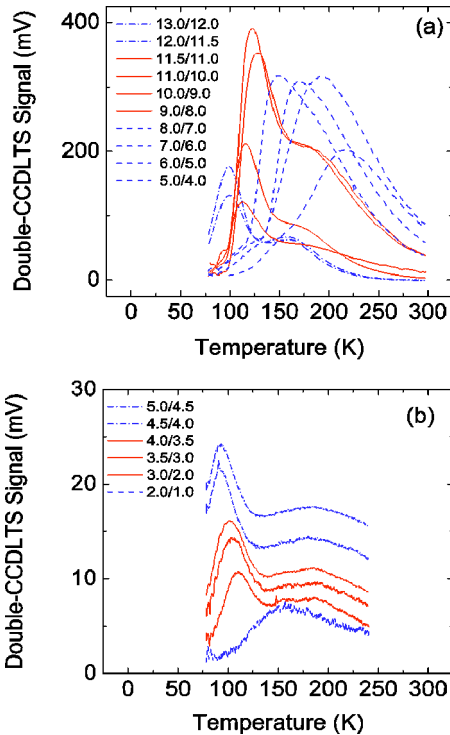


FIG. 5. (Color online) Double-CCDLTS scans for (a) the AO sample and (b) the NO sample at the filling voltages indicated. Scans for the latter are offset vertically. The constant capacitance was 42 pF for the AO sample and 18 pF for the NO sample. The filling pulse duration is 20 ms, and the rate window is 8.6 ms.

and the emission activation energy and capture cross sections were determined from Arrhenius plots in the usual way.⁸ The thermal emission of electrons from a deep level is described by $e_n = v_n \sigma_n N_C \exp[-E_a/kT]$, where e_n is the emission rate, σ_n is the capture cross section, v_n is the thermal velocity, k is the Boltzman constant, N_C is the effective density of states in the conduction band, and T is the temperature of the CCDLTS or double-CCDLTS peak. E_a is the emission activation energy, which for most deep levels is equal to the energy difference between the trap and the bottom of the conduction band, $E_C - E_0$. Substituting $v_n = \sqrt{3kT/m^*}$ and $N_C = 2(2\pi m^* kT/h^2)^{3/2}$, where $m^* = 0.36m_0$ (from Ref. 13) is the density of states effective mass, the temperature dependence of the emission rate is

$$\ln\left(\frac{e_n}{T^2}\right) = -\frac{(E_C - E_0)}{k} \frac{1}{T} + \ln\left(\frac{4\sqrt{6}\pi^{3/2} m^* k^2}{h^3} \sigma_n\right).$$

Thus, the energy position of the interface states is determined from the slope of the Arrhenius plot of $1000k \ln(e_n/T^2)$ versus $1000/T$ and the capture cross section, σ_n , is obtained from the intercept. The uncertainty in the emission activation energy is typically 0.02 eV and in the capture cross section it is an order of magnitude. As examples, Fig. 6(a) shows a plot for each of the three groups of double-CCDLTS peaks for the AO sample. Arrhenius plots for the NO sample are shown in Fig. 6(b). Data for the higher temperature peaks in the NO sample are from CCDLTS scans taken at different rate windows, since the intensity of the signal was too weak to obtain double-CCDLTS data for these traps.

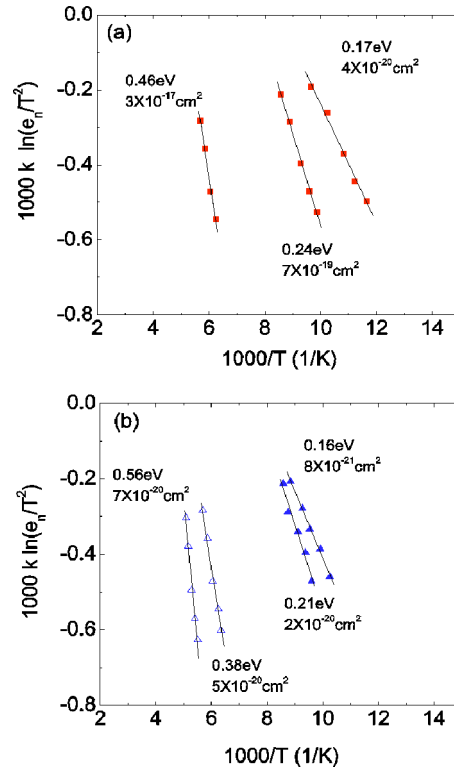


FIG. 6. (Color online) Arrhenius plots: (a) representative data from double-CCDLTS scans for the AO sample with filling pulse voltages 7.0/6.0, 10.0/9.0, and 13.0/12.0 V at constant capacitance 42 pF and (b) double-CCDLTS data for the NO sample with pulse voltages 3.5/3.0 and 5.0/4.5 V at constant capacitance 18 pF and CCDLTS data (open symbols) with filling pulse voltage 5 V.

Figure 7 shows the capture cross section plotted as a function of the activation energy. The three distinctly different values for the capture cross section, ranging from 5×10^{-17} to 5×10^{-20} cm², clearly demonstrate that three different species of interface traps are present in the AO samples: (1) centered at $E_C - 0.46$ eV, with a capture cross section of 4×10^{-17} cm²; (2) centered at $E_C - 0.24$ eV, with $\sigma = 7 \times 10^{-19}$ cm²; and (3) centered at $E_C - 0.17$ eV with $\sigma = 4 \times 10^{-20}$ cm². The behavior of group 1 and 2 states, which dominate the CCDLTS spectra of the AO samples, is as ex-

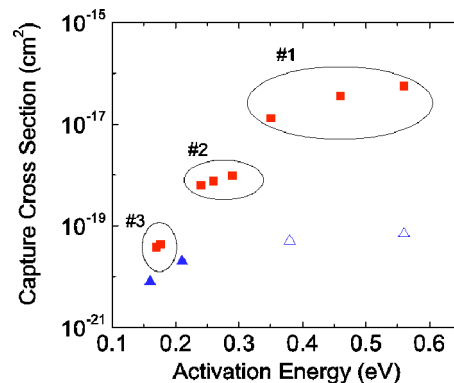


FIG. 7. (Color online) Capture cross section and emission activation energy determined from double-CCDLTS (solid symbols) and CCDLTS (open symbols) measurements for the AO (squares) and the NO (triangles) samples. The uncertainty in the activation energy is 0.02 eV and it is an order of magnitude in the capture cross section.

pected for a continuous distribution of interface states.⁸ A prior CCDLTS study of dry-oxidized *n*-type 4H-SiC MOS capacitors shows the presence of two types of interface states with electron capture cross sections estimated to be $<10^{-16}$ cm² (fast) and $<10^{-19}$ cm² (slow), consistent with our results.¹⁰

Two distributions of states are observed by double-CCDLTS in NO samples: one centered at $E_c-0.21$ eV, with $\sigma=2\times 10^{-20}$ cm², and another at $E_c-0.16$ eV, with $\sigma=8\times 10^{-21}$ cm². The fixed peak position of the $E_c-0.16$ eV distribution with increasing filling voltage is the same as was observed for the $E_c-0.17$ eV (group 3) traps in the AO sample. This anomalous behavior and the similar values of the emission activation energy and capture cross section indicate that these states are near-interface oxide traps, which are present in both samples but with vastly different densities. The temperature shift with increasing filling voltage of the $E_c-0.21$ eV group is consistent with a continuous distribution of interface states.

Parameters for the deeper states at $E_c-0.38$ eV, with $\sigma=5\times 10^{-20}$ cm², and at $E_c-0.56$ eV, with $\sigma=7\times 10^{-20}$ cm² in the NO samples were obtained from CCDLTS spectra. Thus, for these trap distributions we cannot distinguish between states located precisely at the interface or near-interface states. Note that all the interface states in the NO samples have very small capture cross sections, in the range $10^{-21}-10^{-19}$ cm², suggesting possible capture to a negatively charged state,¹⁴ i.e., that these states may be double acceptors. These results clearly show that the two dominant species of interface states observed in the AO samples, electron traps having capture cross sections 4×10^{-17} and 7×10^{-19} cm², are completely passivated by annealing in NO. The density of the third species, centered at $E_c-0.17$ eV having a capture cross section 4×10^{-20} cm² and apparently not located precisely at the interface, is significantly reduced as well. Note that the capture cross section reported for this third trap species represents only a small fraction of all the defects in this energy range.

E. Comparison of D_{it} from DLTS and $C-V$ measurements

With the capture cross sections of the different trap species established, D_{it} can be calculated from the CCDLTS data.⁷ For electron emission from a continuous distribution of interface states, the CCDLTS signal $\Delta V_G = qkT \ln(t_2/t_1) D_{it}(E_o)/C_{ox}$ is proportional to the interface-state intensity $D_{it}(E_o)$, where E_o is in the semiconductor band gap, q is the electronic charge, k is the Boltzmann constant, and C_{ox} is the oxide capacitance. The ratio t_2/t_1 is determined by the CCDLTS system rate window setting. When the capture cross section is independent of temperature, the CCDLTS signal temperature is related to the emission activation energy by $1/\tau_n = \sigma_n v_n N_C \exp(-\Delta E/kT)$, where $1/\tau_n$ is the emission rate determined by the rate window selected for the CCDLTS scan, σ_n is the capture cross section, v_n is the electron thermal velocity, and $\Delta E = E_c - E_o$, where E_c is the energy of the bottom of the conduction band of 4H-SiC. Since the capture cross sections of the three species of traps

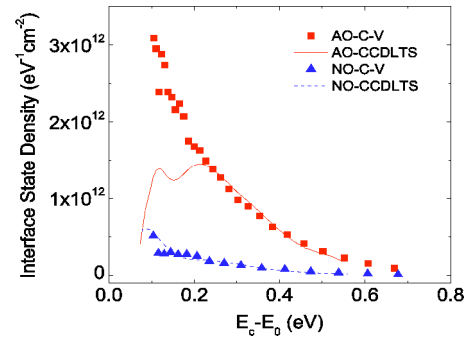


FIG. 8. (Color online) Distribution of SiO₂/4H-SiC interface states obtained from CCDLTS and high-low $C-V$ measurements on AO and NO samples.

present in the AO samples are different, the energy distribution of each trap species must be calculated separately. This was accomplished by fitting the CCDLTS spectrum to the sum of three Gaussian distributions with peak temperatures of 198, 128, and 93 K for groups 1, 2, and 3 respectively. The fit to the CCDLTS data and the three Gaussian curves representing the three trap distributions are shown in Fig. 4(a). The energy was calculated for each trap distribution using capture cross section values of 4×10^{-17} , 7×10^{-19} , and 4×10^{-20} cm² for traps 1, 2, and 3, respectively. The capture cross sections were assumed to be independent of temperature, consistent with the data in Fig. 7. A single capture cross section, the midrange value of 2×10^{-20} cm², was used to convert temperature to energy for the NO sample.

Figure 8 shows the calculated D_{it} profile obtained from the CCDLTS measurements for both the AO and NO samples. For comparison, the D_{it} determined from the room temperature high-low frequency $C-V$ measurements of these samples is also shown. The D_{it} obtained from CCDLTS data for the NO sample agrees well with the density obtained from the $C-V$ technique. In contrast, the agreement is good only for energy >0.2 eV for the AO sample. The D_{it} extracted from the high-low frequency $C-V$ measurements of the same capacitor increases strongly close to the conduction band edge, in agreement with previous observations.¹⁵ However, the decreasing CCDLTS signal at $T < 110$ K is in agreement with previous CCDLTS,¹⁰ thermally stimulated current,¹¹ and thermal dielectric relaxation current¹² results on SiO₂/4H-SiC MOS structures. This discrepancy suggests that the large density of interface states lying close to the conduction band edge in the AO samples is not accessible on the time scale of the CCDLTS measurement. We note that, because the traps are filled at constant applied voltage and the AO sample exhibits a large shift of the flatband voltage with decreasing temperature, the electric field also decreases with temperature. The lower electric field at low temperature might also explain the discrepancy in the D_{it} , even though the CCDLTS spectra appear to saturate within the available range of filling voltages, as shown in Fig. 2(a). The need for a higher electric field or a longer duration filling pulse to trap electrons suggests that these states may lie within the oxide layer, rather than at the SiO₂/SiC interface. In that case capture would be via tunneling and the capture rate would be significantly slower than that for states at the interface.

IV. DISCUSSION

It is interesting to comment on these results in light of current models of the SiO₂/SiC interface. Earliest models^{16,17} attributed the large accumulation of defects near the conduction band to carbon or carbon clusters with energy level spanning the bottom of the conduction band of 4H-SiC. This explanation elegantly and simply explained the large difference between the defect density near E_c for the 6H and 4H polytypes. Chung *et al.* quantified and extended this model in terms of cluster size and placement within the gap.³ Their results indicate a distribution of defects, with isolated carbon atoms deep in the gap and larger clusters closer to the band edge. The role of nitrogen was then envisioned to “pair” with carbon, totally eliminating isolated carbon-induced defects and reducing existing clusters to still smaller number of carbon atoms. Some experimental support for this picture arises through the work of McDonald *et al.*, who showed that the kinetics associated with the elimination of defects with nitrogen additions was consistent with a model consisting of isolated carbon atoms deep in the gap and clusters closer to the conduction band edge.⁴ Nevertheless, the absolute identification of carbon clusters at the interface remains problematic, although recent surface enhanced Raman spectroscopy (SERS) results come closest to the requisite sensitivity.¹⁸ Indeed some of the defects may be SiCO complexes of various sizes as well as the expected dangling bond type defects associated with simple silicon structures. In addition the presence of near-interface states in the SiO₂ layer, in lower concentration than carbon clusters, has also been demonstrated.^{17,19}

These new CCDLTS results can be interpreted in light of the cluster and isolated atom model. Isolated atoms, deep in the gap, can be expected to have rather large capture cross sections, comparable to the dangling bond cross sections associated with P_b centers in silicon. Indeed capture cross sections for interface states in SiO₂/Si have recently been measured in the range 1×10^{-18} – 1×10^{-16} cm² with states deeper in the gap having larger capture cross sections than those lying closer to the conduction band edge.⁹ The large nitrogen-induced change in defect cross section deep in the gap reported here suggests that nitrogen passivates these large capture cross section defects. The remaining defects are of an entirely different nature. Possibly the isolated defects are eliminated, and relatively inert clusters remain. In this picture the near edge defects are a conglomeration of clusters, and are effectively reduced (dissolved) by nitrogen, but not totally eliminated. The dissolved clusters give rise to more isolated species, passivated by nitrogen. Other clusters, evidently not susceptible to nitrogen dissolution, remain in the material. Evidence for interfacial clusters and their reduction by nitridation has recently been supported by SERS experiments.¹⁸ In the same sense the nitrogen may “totally” remove the isolated carbon deep in the gap. The deeper interface defects remaining after nitridation are of a very different character, possibly clusterlike, and can be the focus of further improvements in the interface.

The smaller change in cross sections observed closer to the band edge suggests that nitrogen has a smaller effect in

changing the nature of the defect in this energy region. High-low frequency $C-V$ measurements show that the absolute magnitude of the defect reduction is greatest near the band edge. The inability to detect the majority of the passivated traps with energy $<E_c-0.2$ eV by CCDLTS suggests that the remaining defects in this energy range are different in character as well. The small values of the capture cross section of the residual defects in the energy range near $E_c-0.1$ eV is consistent with near-interface traps in the oxide, whose density is also significantly reduced by NO annealing, in agreement with the model of Ref. 4.

V. CONCLUSIONS

CCDLTS measurements of the capture and emission characteristics of as-oxidized and NO annealed SiO₂/4H-SiC MOS capacitors demonstrate the presence of several different types of interface states, distinguished by their different capture cross sections and response to nitridation. These are: (i) a large density of relatively deep interface states having capture cross sections in the range 5×10^{-19} – 1×10^{-16} cm² that are fully passivated by NO annealing, (ii) near-interface states, which have even smaller capture cross sections ($\sim 10^{-21}$ cm²), that are partially passivated by NO annealing, and (iii) states that remain after NO annealing, all having capture cross sections in the range of 10^{-21} – 10^{-19} cm². In addition, we find that the largest density of states passivated by NO annealing is not observed using CCDLTS measurements. As discussed earlier these results can be interpreted in terms of models in which the majority of defects at the SiO₂/4H-SiC interface are carbon clusters. Our results also indicate the presence of near-interface states, presumably states in the SiO₂, which are partially removed by NO annealing.

ACKNOWLEDGMENTS

We are grateful to W. Woods in the SFU School of Engineering Sciences for assistance with wire bonding. This work was supported by the National Sciences and Engineering Research Council of Canada, the Canadian Foundation for Innovation, the British Columbia Knowledge Development Fund, the U.S. Army Research Office, the U.S. Army TACOM, and the Defense Advanced Research Projects Agency.

¹R. Schörner, P. Friedrichs, D. Peters, and D. Stephani, IEEE Electron Device Lett. **20**, 241 (1999).

²S. Dhar, S. Wang, L.C. Feldman, and J.R. Williams, MRS Bull. **30**, 288 (2005).

³G. Y. Chung, C. C. Tin, J. R. Williams, K. McDonald, M. Di Ventra, S. T. Pantelides, L. C. Feldman, and R. A. Weller, Appl. Phys. Lett. **76**, 1713 (2000).

⁴K. McDonald, R. A. Weller, S. T. Pantelides, L. C. Feldman, G. Y. Chung, C. C. Tin, and J. R. Williams, J. Appl. Phys. **93**, 2719 (2003).

⁵H. Yano, T. Hirao, T. Kimoto, and H. Matsunami, Appl. Phys. Lett. **78**, 374 (2001).

⁶V. A. Afanas'ev and G. Pensl, Appl. Phys. Lett. **82**, 568 (2003).

⁷N. M. Johnson, D. J. Bartelink, and M. Schulz, in *The Physics of SiO₂ and its Interface*, edited by S. T. Pantelides (Pergamon, New York, 1978), pp. 421–427.

⁸N. M. Johnson, J. Vac. Sci. Technol. **21**, 303 (1982).

⁹T. C. Poon and H. C. Card, J. Appl. Phys. **51**, 5880 (1980).

¹⁰H. Ö. Ölafsson, F. Allerstam, and E. Ö. Sveinbjörnsson, Mater. Sci. Forum

- 389–393**, 1005 (2002).
- ¹¹T. E. Rudenko, I. N. Osiyuk, I. P. Tyagulski, H. Ö. Ólafsson, and E. Ö. Sveinbjörnsson, *Solid-State Electron.* **49**, 545 (2005).
- ¹²E. Pippel, J. Woltersdorf, H. Ö. Ólafsson, and E. Ö. Sveinbjörnsson, *J. Appl. Phys.* **97**, 034302 (2005).
- ¹³N. T. Son, W. M. Chen, O. Kordina, A. O. Konstantinov, B. Monemar, E. Janzén, D. M. Hofman, D. Volm, M. Drechsler, and B. K. Meyer, *Appl. Phys. Lett.* **66**, 1074 (1995).
- ¹⁴A. M. Stoneham, *Theory of Defects in Solids* (Clarendon, Oxford, 1975), p. 520.
- ¹⁵V. V. Afanas'ev, A. Stesmans, M. Bassler, G. Pensl, and M. J. Schulz, *Appl. Phys. Lett.* **76**, 336 (2000).
- ¹⁶V. V. Afanasev, M. Bassler, G. Pensl, and M. J. Schulz, *Phys. Status Solidi A* **162**, 321 (1997).
- ¹⁷M. Bassler, G. Pensl, and V. Afanasev, *Diamond Relat. Mater.* **6**, 1472 (1997).
- ¹⁸S. H. Choi, D. Wang, J. R. Williams, M. Park, W. Lu, S. Dhar, and L. C. Feldman, *Appl. Surf. Sci.* **253**, 5411 (2007).
- ¹⁹V. V. Afanas'ev and A. Stesmans, *J. Phys.: Condens. Matter* **9**, L55 (1997).